

The strength of earthquake-generating faults

Alex Copley

COMET, Bullard Labs, Department of Earth Sciences, University of Cambridge, Cambridge, CB3 0EZ UK
acc41@cam.ac.uk



Abstract: This paper summarizes the observations and methods that have been used to study the strength of active earthquake-generating (seismogenic) faults. Indirect inferences based upon a range of geophysical and geological observations suggest that faults fail in earthquakes at shear stresses of less than *c.* 50 MPa, equivalent to effective coefficients of friction of less than 0.3, and possibly as low as 0.05. These low levels of effective friction are likely to be the result of a combination of high pore fluid pressures, which could be local or transient, and the frictional properties of phyllosilicate-rich fault rocks. The dip angles of new faults forming in oceanic outer rises imply that intrinsically low-friction fault rocks must control the fault strength in at least that setting. When combined with the much higher fault strengths inferred from borehole studies and some laboratory measurements, the observations are most consistent with weak faults embedded in strong surroundings, providing a clear reason for the prevalence of fault reactivation. However, the conditions required for the formation of new faults, and the reasons for an apparent wide variability in the degree of fault healing through time, remain unknown.

Received 10 March 2017; revised 22 June 2017; accepted 22 June 2017

Ever since the realization that faults accommodate the relative motions of parts of the Earth's lithosphere, there has been controversy about their material properties. A major question that has received much attention concerns understanding the friction laws that determine why some parts of faults break in earthquakes whereas others slide aseismically, and equivalently what controls whether a slip event becomes an earthquake or a longer phase of transient aseismic creep (e.g. Dietrich 1979; Ruina 1983; Marone 1998; Scholz 1998). A component of this question involves establishing whether a given fault always behaves in the same manner. Observations from regions where suitably old markers of fault motion, or long historical records, give a view of multiple earthquake cycles suggest two important features. One is that at the scale of entire fault zones, some regions appear to be persistently seismic, and are locked and accumulating strain in the interseismic period, whereas others show little evidence of generating significant earthquakes (e.g. Ambraseys & Jackson 1998; Sieh *et al.* 2008; Chlieh *et al.* 2011). Such patterns exist on a larger scale than the dynamic propagation of seismic slip into creeping regions on the margins of individual slip patches, and the geometrical details around the boundaries between these regions are not well known. A second feature is that, with some exceptions, the slip areas and magnitudes of earthquakes usually appear to vary between successive seismic cycles on a given fault system, possibly as a result of stress perturbations from previous motions (e.g. Beck *et al.* 1998; Scholz 1999; Konca *et al.* 2008; Kozaci *et al.* 2010).

A second major question concerns the levels of stress that faults can support before moving by either seismic slip or aseismic creep. This paper focuses on this second question, and addresses the magnitude of differential stress required to cause earthquake-generating faults to slip. The particular focus on seismogenic faults, rather than creeping faults, is because a wealth of information revealed by studies of earthquakes can be incorporated into the analysis. Whereas a large body of work is devoted to the evolution of friction during the process of fault slip (e.g. Rice 2006; Reches & Lockner 2010; Di Toro *et al.* 2011; Brown & Fialko 2012; Noda & Lapusta 2013, and references therein), this paper concentrates on the 'static' friction that needs to be overcome to begin the process of fault motion, and not the subsequent evolution of material

properties during a seismic event. The level of differential stress required to begin the process of earthquake slip is often known as the fault 'strength'.

The determination of fault strength has a number of wide-ranging implications. One of these relates to the rheology of the continental lithosphere, and its control on the locations and characteristics of deformation. There has been plentiful recent debate surrounding the relative magnitudes of the stresses transmitted through the brittle and ductile parts of the lithosphere, and how these stresses relate to the lateral variations of continental rheology that play a major role in controlling the geometry and rates of deformation (e.g. Watts & Burov 2003; Jackson *et al.* 2008; Burov 2010; Copley *et al.* 2011a). To fully address this question requires an understanding of the level of stress that can be supported by seismogenic faults.

A second major implication of the strength of active faults relates to earthquake recurrence and hazard. Earthquake stress drops are commonly of the order of megapascals to tens of megapascals (e.g. Kanamori & Anderson 1975; Allmann & Shearer 2009). Opinion is divided as to whether or not these values represent the total pre-earthquake shear stress on fault planes (e.g. Kanamori 1994; McGarr 1999; Scholz 2000; Townend & Zoback 2000; Copley *et al.* 2011a). If earthquake stress drops do represent the release of the great majority of the pre-event shear stresses on fault planes (so-called 'weak faults'), then a significant time interval will be required for stresses to build up again before an earthquake can nucleate on a previously ruptured fault segment. If the tectonic loading rate is roughly constant, and in the absence of interactions with other faults, this situation may lead to quasi-periodic ruptures on a given fault segment. If, however, earthquake stress drops represent only a small proportion of the pre-earthquake shear stresses on fault planes (so-called 'strong faults'), then unreleased shear stresses will be present following earthquakes, which could lead to events closely spaced in time. Understanding the stress state of faults therefore has significant implications for hazard assessment.

This paper will begin by describing the range of methods that have been used to estimate the stress state at failure of active faults, and then combine these results into a coherent overall view of fault strength.

Direct observations

One of the earliest, and most developed, lines of argument relating to fault strength is based on the mechanical testing of rocks. These methods can be subdivided into those where specimens are tested in laboratories and *in situ* experiments undertaken in boreholes.

Laboratory experiments

Byerlee (1978) represents one of the most influential studies in fault mechanics. Clean saw-cuts through samples of a wide variety of rock types were loaded, and the stress levels at which they slipped were used to define a failure criterion for the rocks. Known as 'Byerlee's Law', this criterion suggests that the coefficient of friction (the ratio of the shear stress to the normal stress at failure) is between 0.6 and 0.85, depending upon the confining pressure. This result was independent of rock type for most samples, but clay minerals were seen to have lower coefficients of friction than implied by the law, as discussed below. When applied directly to the Earth, Byerlee's Law implies differential stresses in the mid- to lower crust (in places where it is seismogenic) of over 500 MPa (Fig. 1), and so suggests that earthquake stress drops (commonly megapascals to tens of megapascals (e.g. Kanamori & Anderson 1975; Allmann & Shearer 2009)) represent the release of only a small proportion of the total shear stress on faults.

However, there are some difficulties involved in applying Byerlee's Law directly to the Earth. The first of these relates to the pore fluid pressure. Fluids in fault zones could be derived from a range of sources, such as the surface hydrosphere, metamorphic dehydration reactions, sediment compaction, and flux from the mantle. High-pressure fluid in pores on faults acts to locally reduce the effective normal stress, and means that for a given coefficient of

friction the faults will be able to fail at lower shear stresses than if the fluid were absent. The pore fluid pressure at seismogenic depths within the Earth is not well known. Measurements from a variety of deep boreholes have been used to suggest dominantly hydrostatic pore pressures (e.g. Townend & Zoback 2000, and references therein). However, observations and models of extensional veins and joints produced by natural hydrofracture (e.g. Secor 1965; Ramsay 1980; Sibson 1994; Robert *et al.* 1995; Barker *et al.* 2006) imply that at least in some places, and at some times, fluid pressures must be greater than the minimum principal compressive stress (with the possibility of variation over multiple timescales, including individual earthquake cycles). Observations of extensional veining in regions of horizontal shortening, where this minimum principal stress is vertical, therefore imply fluid pressures of greater than the lithostatic pressure (e.g. Sibson 2004). The precipitation of gold into some of these extensional veins suggests that these high fluid pressures must persist for long enough, although not necessarily continuously, for significant volumes of fluid to pass through the open fractures (e.g. Robert *et al.* 1995) (10^9 m³ of fluids are required to precipitate 10 tonnes of gold; Steward 1993; Sibson 2004).

The spatial and temporal variability of pore pressures within the Earth may depend on tectonic, geological and metamorphic setting (e.g. Sleep & Blanpied 1992; Sibson 2014). The compaction of fluid-filled sediments can easily lead to fluid pressures of greater than hydrostatic if impermeable horizons are present in a sedimentary sequence (e.g. Smith 1971; Osborne & Swarbrick 1997). Dehydration reactions during prograde metamorphism will be likely to generate fluid pressures of close to, or greater than, the lithostatic pressure (e.g. Walther & Orville 1982; Yardley 2009). For externally derived fluids to generate high pore pressures requires both permeable rocks to allow ingress of the fluids, and an impermeable seal to allow the fluid pressure to rise above

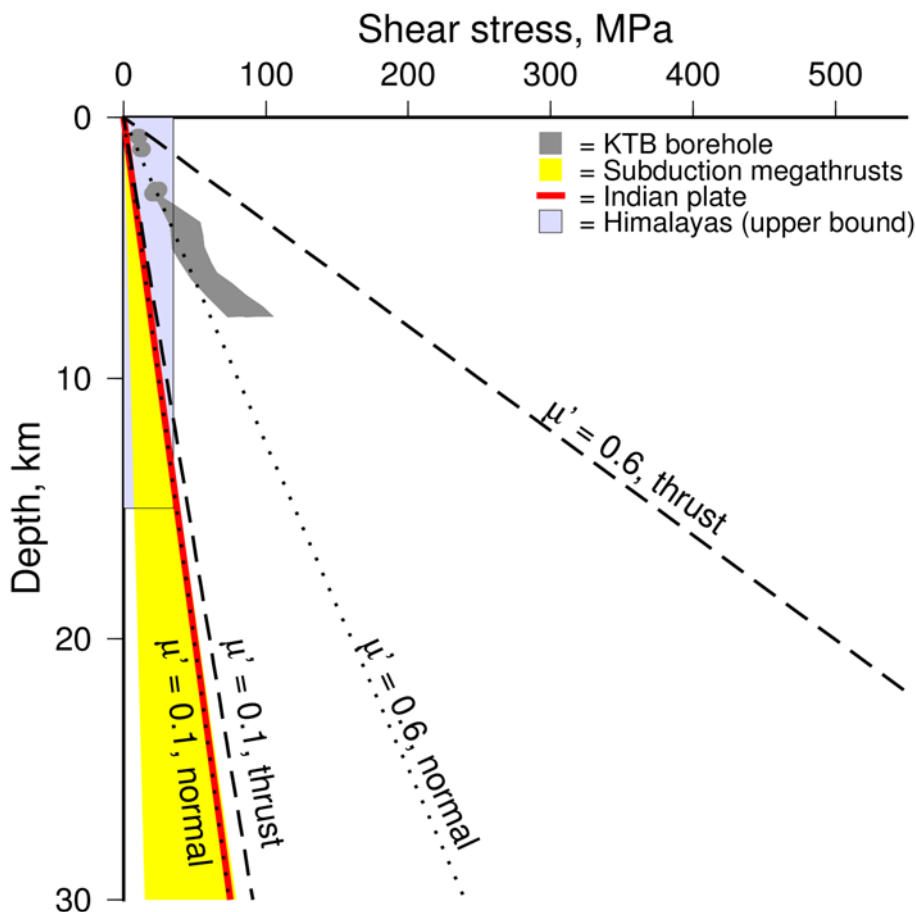


Fig. 1. Estimates of shear stress as a function of depth from various sources. The grey polygon represents the estimate from the KTB borehole by Brudy *et al.* (1997), converted from differential stress by assuming the faults strike at 45–60° to the orientation of the maximum principal stress. The red line represents the suggestion of Copley *et al.* (2011a) for the Indian Shield, and the yellow shaded region encompasses the estimates of Lamb (2006) for subduction-zone megathrusts. The blue rectangle represents a maximum vertically averaged value for the Himalayan thrust faults, based upon Bollinger *et al.* (2004) and Copley *et al.* (2011b). The dashed and dotted lines show predictions calculated for effective coefficients of friction (μ') of 0.6 and 0.1, for reverse-faulting and normal-faulting settings.

hydrostatic. Under certain conditions fault zones (e.g. Faulkner *et al.* 2010) and underlying ductile shear zones (e.g. Beach 1980) can act as fluid pathways (e.g. as suggested by Diener *et al.* (2016) for the influx of fluid during retrograde metamorphism in a mid-crustal shear zone cutting dry granulites). A further effect of fluid flow along faults is related to chemical reactions. Extensive fluid–rock reaction can produce layers of phyllosilicates, which can significantly weaken fault zones, as discussed below (e.g. Wintsch *et al.* 1995; Imber *et al.* 1997).

A second difficulty in applying Byerlee’s Law to the Earth relates to the composition of fault rocks. Experiments on phyllosilicates (such as the clays commonly found in exposed faults) show them to have much lower coefficients of friction than crystalline rocks (e.g. Byerlee 1978; Saffer *et al.* 2001; Brown *et al.* 2003). Given that roughly two-thirds of the world’s sedimentary rock record is mudrocks (e.g. Ilgen *et al.* 2017), these low coefficients of friction are likely to be relevant to the upper crust in many regions. Laboratory tests on samples collected from exposed faults, and from boreholes that intersect faults (so far limited to the top few kilometres of the crust), often imply low coefficients of friction for the fault rocks (e.g. Collettini *et al.* 2009; Lockner *et al.* 2011; Remitti *et al.* 2015). These results imply that once a fault has developed a phyllosilicate-rich core, its strength will dramatically reduce. The probable mechanical differences between intact rock and phyllosilicate-rich faults will be discussed further below.

An over-arching question relating to laboratory experiments that study rock friction relates to the applicability of those results to Earth conditions. For practical reasons the rate of stressing of laboratory samples is much higher, and the size of samples is much smaller, than natural fault surfaces capable of producing large earthquakes. Additional difficulties are presented by the laboratory experiments not being able to reproduce the (unknown) hydrological conditions on natural faults, and long-term processes such as mineral precipitation and dissolution. The importance of these mismatches between the experiments and the natural world remains to be assessed, but could be addressed if the material properties of natural faults can be estimated by independent means, for comparison with the laboratory results.

Borehole results

In situ down-borehole experiments provide a second means of directly measuring fault properties. Methods of estimating the magnitudes and orientations of stresses in boreholes have been reviewed by Zoback *et al.* (2003). The major methods entail observations of borehole deformation (compressive breakouts and tensile fractures) and the formation of new fractures by elevating borehole fluid pressures. A series of results from the deepest boreholes yet studied with these methods (up to *c.* 8 km) resulted in a consistent picture where the stresses required to cause rock failure are consistent with coefficients of friction of 0.6–1.0 and hydrostatic pore-fluid pressures (grey shaded area in Fig. 1; e.g. Zoback & Healy 1992; Brudy *et al.* 1997; Lund & Zoback 1999). These results are consistent with the laboratory-derived Byerlee’s Law. The agreement between boreholes, and with Byerlee’s Law, apparently implies that the measurements are accurately capturing the stresses required to generate new faults and tensile fractures using the down-borehole methods. However, uncertainty remains over whether these observations are representative of faulting in geological conditions. The borehole results involve the observation of small fractures that are newly formed by drilling and by fluid pressure increases. The fluid-induced fractures are dilatational, whereas major earthquakes are shear failures. The time- and length-scales involved in borehole experiments are orders of magnitude smaller than those of natural faulting in large earthquakes. It is therefore an open question whether these borehole results accurately

represent the properties of crustal-scale faults failing by shear on pre-existing surfaces on the timescales of earthquake cycles.

The ‘direct’ measures of fault friction can therefore be seen to provide a detailed view of the behaviour of natural and synthetic faults and rocks on short time- and length-scales. However, the uncertainties involved in the extrapolation to geological conditions mean that we also need to consider indirect inferences of the properties of natural faults in order to develop a complete picture of fault rheology and behaviour.

Indirect inferences

A second set of arguments relating to fault properties has been constructed based on observations that can be analysed to infer fault strength, rather than measure it directly (e.g. using heat flow, force balance calculations or the orientation of strain). Although these methods do not directly measure the rock properties, and so are at a disadvantage compared with the methods described above, their advantage is that they analyse natural faults under geological conditions.

Thermal arguments

The amount of work done against friction by fault motion controls the rate of heat production along a fault plane. The rate of heat production is given by $H = \tau v/w$ (e.g. Sibson 1977), where H is the rate of heat production, τ is the shear stress on the fault, v is the slip rate and w is the thickness of the fault zone. An important feature of this equation is that it shows the rate of heat production to depend on the total shear stress on the fault, and so provides a method to estimate this quantity when combined with a model for heat transport through the crust and surface heat-flow measurements or thermochronological cooling ages. An early example was from the San Andreas Fault, where the lack of a significant heat-flow anomaly over the fault was taken to indicate low fault friction (with a shear stress on the fault of less than a few tens of megapascals, equivalent to an effective coefficient of friction of ≤ 0.3) (e.g. Brune *et al.* 1969; Lachenbruch & Sass 1980; Lachenbruch & McGarr 1990). Similar arguments have been used in the Himalaya, where the distribution of mineral cooling ages measured by low-temperature thermochronology suggests minimal heat production on the Himalayan megathrust, and so a low effective coefficient of friction (Herman *et al.* 2010). Equivalent results have been inferred from heat-flow measurements above subduction-zone megathrusts (Gao & Wang 2014). However, caution must be exercised because of the unknown fluid flow and hydraulic connectivity along and around faults. Significant heat could be advected by fluid flow along, or away from, faults. Such a process would alter the thermal structure away from predictions calculated assuming heat transport only by advection and diffusion in the solid Earth. Assumptions about fluid flow also affect in a similar way the interpretation of the lack of major thermal anomalies on faults that have been drilled following major earthquakes (Fulton *et al.* 2013; Li *et al.* 2015). The widespread presence of hot springs along active faults in the continents, and of black smokers along mid-ocean ridges, shows that fluid circulation commonly occurs near faults, and that it transports heat (e.g. Rona *et al.* 1986; Hancock *et al.* 1999).

A second thermal consideration relates to the production of pseudotachylytes. These are crystallized (quenched) sheets of melt produced by fault motion (e.g. Scott & Drever 1954; Sibson 1975). For melting to occur on a fault plane, McKenzie & Brune (1972) suggested that the earthquake slip must satisfy the condition $A \leq \tau^2 D$, where τ is the shear stress, D is the amount of fault slip and A is a constant that depends upon the material properties of the rock, including the melting temperature. A lower bound on fault friction

can therefore be estimated by calculating the amount of heat production that would be required to melt the rocks along a fault plane. This lower bound implies that fault strength must be of the order of megapascals or greater (e.g. McKenzie & Brune 1972), in agreement with the observed stress drops in earthquakes (e.g. Kanamori & Anderson 1975; Allmann & Shearer 2009), although some higher estimates of the required shear stress do exist (e.g. >100 MPa; Sibson & Toy 2006). McKenzie & Brune (1972) further argued that the production of a lubricating sheet of melt on the fault would remove its ability to support significant shear stresses, and that the earthquake stress drops should therefore represent the release of the total pre-earthquake shear stress on the fault. However, questions remain regarding whether entire fault surfaces form pseudotachyrites during slip, or only localized asperities (in which case the remainder of the fault could continue to support stresses after an earthquake). In addition, the relatively small and discontinuous field outcrops of pseudotachyrites often do not allow the amount of slip to be estimated (D in the equation above), which leads to a trade-off with the shear stress on the fault plane. Also, it is not accurately known whether the viscosity of the melts is low enough that the assumption of complete lubrication and stress release is accurate (e.g. Scholz 1990; Spray 1993).

Studies of the thermal effects of faulting are therefore often used to suggest that active faults slip at relatively low shear stresses (tens of megapascals at most), but because of the uncertainties described

above these methods cannot provide a conclusive estimate of fault strength.

Fault dips

The use of the dips of dip-slip earthquake fault planes to estimate fault strength is controversial. The optimal dip angle at which a fault is formed, or reactivated, depends upon the coefficient of friction of the rocks, and is unaffected by the pore fluid pressure (although this will affect the absolute magnitude of the stress at which faulting occurs) (Fig. 2; e.g. Sibson 1985; Middleton & Copley 2014). Fault dip angles are usually interpreted in the framework of ‘Andersonian’ fault mechanics (Anderson 1951), in which the absence of significant shear stress on the Earth’s surface is assumed to result in one of the principal stresses being vertical in orientation. The dips of normal-faulting earthquake nodal planes are seen to concentrate around 45° , with upper and lower limits at $\sim 60^\circ$ and $\sim 30^\circ$ (Fig. 2; e.g. Jackson & White 1989). Earthquake nodal plane dips estimated by modelling P- and SH-waveforms are commonly accurate to $\pm 5\text{--}10^\circ$ (e.g. Molnar & Lyon-Caen 1988; Taymaz *et al.* 1991; Craig *et al.* 2014b), so the features of the dip distribution are well resolved, although this accuracy limits the resolution of subsequent estimates of the coefficient of friction.

Thatcher & Hill (1991) and Collettini & Sibson (2001) interpreted the dip distribution of normal-faulting earthquake fault

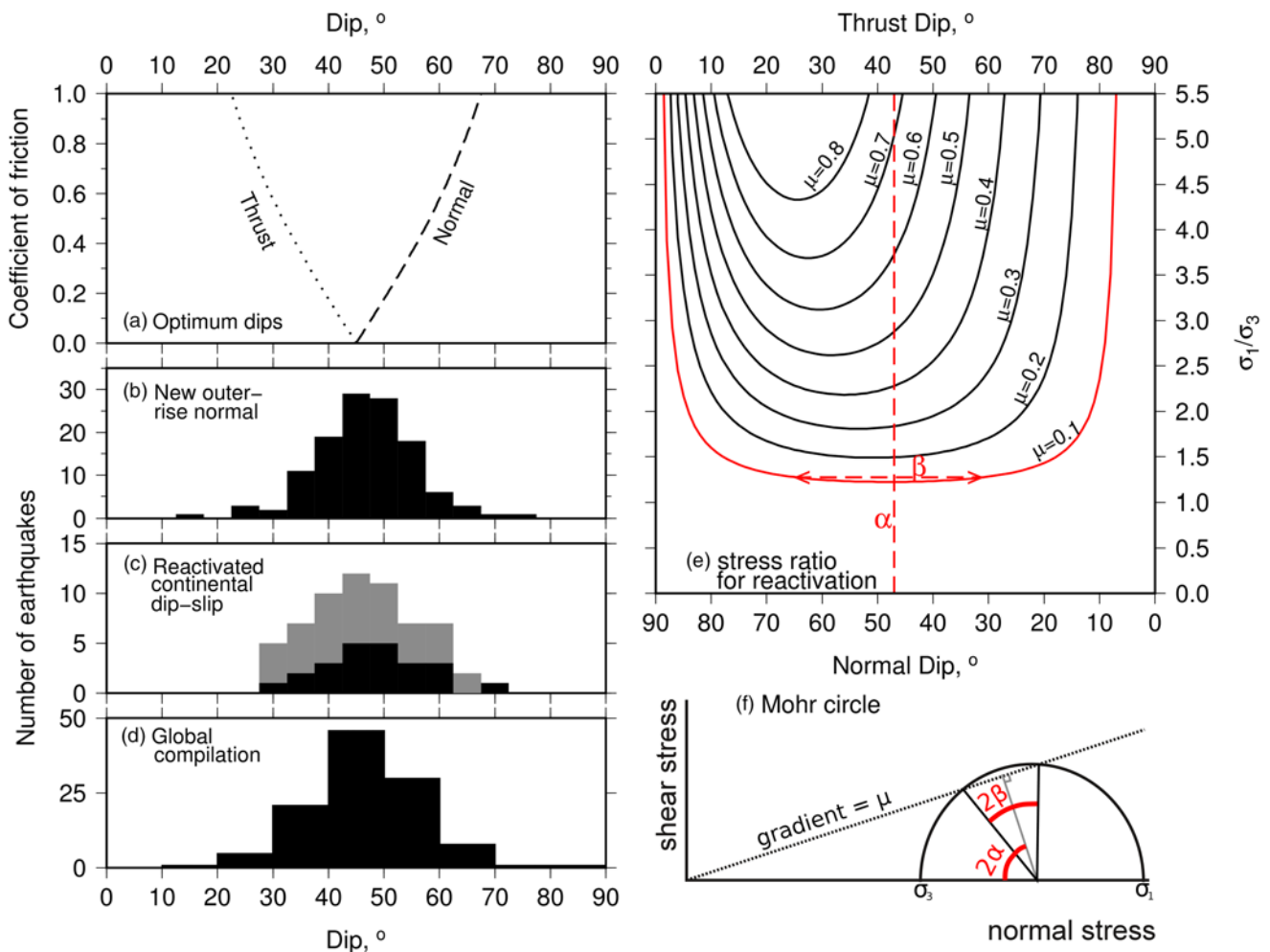


Fig. 2. (a) Optimum dip angles of reverse and normal faults, as a function of the coefficient of friction. The histograms show observed earthquake nodal plane dips in (b) earthquakes on new normal faults forming in oceanic outer rises (Craig *et al.* 2014a), (c) earthquakes on reactivated continental dip-slip faults (Middleton & Copley 2014; black are normal faults, grey are reverse faults), (d) earthquakes in a global compilation of normal faults (Jackson & White 1989). (e) Ratio of the maximum and minimum principal stresses required to reactivate a dip-slip fault of a given dip and coefficient of friction (Sibson 1985). (f) Mohr circle representation of fault reactivation, schematically showing the angles α and β indicated in (e).

planes to represent fault formation at 60°, followed by rotation through displacement accumulation to 30°, at which point frictional lock-up occurs (although some reactivation of thrust faults was also envisaged, and Thatcher & Hill (1991) also raised the possibility of the dip angles being controlled by the ductile behaviour of the lower crust). Such an interpretation implies a coefficient of friction of *c.* 0.6, although it does not provide an explanation for the concentration of dips at around 45°, only the values of the end-points of the distribution. Sibson & Xie (1998) suggested an equivalent interpretation to explain the dips of reverse-faulting earthquake fault planes. Middleton & Copley (2014) proposed an alternative view, in which the coefficient of friction is ≤ 0.3 , resulting in the concentration of dips close to 45°, which is the optimum angle of fault formation and reactivation at low coefficients of friction (α in Fig. 2). In their interpretation, the end-points in the dip distribution depend upon the strength and distribution of pre-existing weak planes within the lithosphere, which can fail in preference to more optimally oriented planes (β in Fig. 2). If Middleton & Copley (2014) are correct, the observed range of dips would imply these weak zones are at least 30% weaker than intact rock (Copley & Woodcock 2016). The interpretation of the earthquake dip distributions therefore rests on whether the concentration of dips at $\sim 45^\circ$, which is statistically significant, is viewed as an important feature that needs to be explained. The seismological results of Craig *et al.* (2014b), which show that new normal faults in oceanic outer rises form at dip angles of close to 45°, appear to confirm the presence of intrinsically low-friction material along faults in at least that geological setting.

Stress and strain orientations

Mount & Suppe (1987) described how the orientations of principal stresses with respect to faults can be used to infer the fault frictional properties. They suggested that the San Andreas Fault must represent an almost frictionless surface, because borehole breakouts and the orientations of anticlines imply that the maximum horizontal compressive stress is close to perpendicular to the fault. However, estimates of the stress orientation in the absence of

major topographic features (as described below) are fraught with difficulties. The maximum horizontal compressive stress can lie anywhere within the compressive quadrant of earthquake focal mechanisms (McKenzie 1969). Borehole breakout observations can give the orientation of the maximum principal stress at shallow depths, but in places this can be incompatible with that at seismogenic depths (e.g. as can be seen by comparing the results of Gowd *et al.* (1992) and Chen & Molnar (1990)), presumably because of decoupling horizons in the shallow crust. Miller (1998) suggested that the folds flanking the San Andreas Fault originally formed at an angle of 20–30° to the fault and have since been rotated to be fault-parallel, showing the difficulties of using geological structures to estimate stress orientations. Additionally, it has been suggested that the orientations of principal stresses may change close to faults, rather than being homogeneous over wide deformation zones (e.g. Scholz 2000).

In contrast to the orientation of stress, measurements of the orientation of strain can be directly obtained from earthquake slip directions (i.e. the orientation of the focal mechanism of an earthquake). To use the orientation of strain to estimate fault strength, it is also necessary to know the orientation and magnitude of the forces driving the deformation, which is more difficult. For example, in a linear mountain range, compression due to plate convergence across the range, and gravitational potential energy contrasts resulting from crustal thickness contrasts (which result in a buoyancy force; Fig. 3), can both exert forces in the same direction. Although the magnitude of gravitational potential energy contrasts can be estimated from the crust and upper mantle structure (e.g. Artyushkov 1973; Dalmayrac & Molnar 1981; England & Houseman 1988; England & Molnar 1997), the forces due to the plate convergence are more difficult to estimate, and in many locations are not well known. In such a linear mountain range, there will therefore be a trade-off between the estimated force required to break the faults in earthquakes, and the magnitude of the compressive forces due to the plate convergence.

By studying mountain ranges that are curved in plan view, it is possible to remove this trade-off. In a curved mountain range, the forces resulting from gravitational potential energy contrasts will

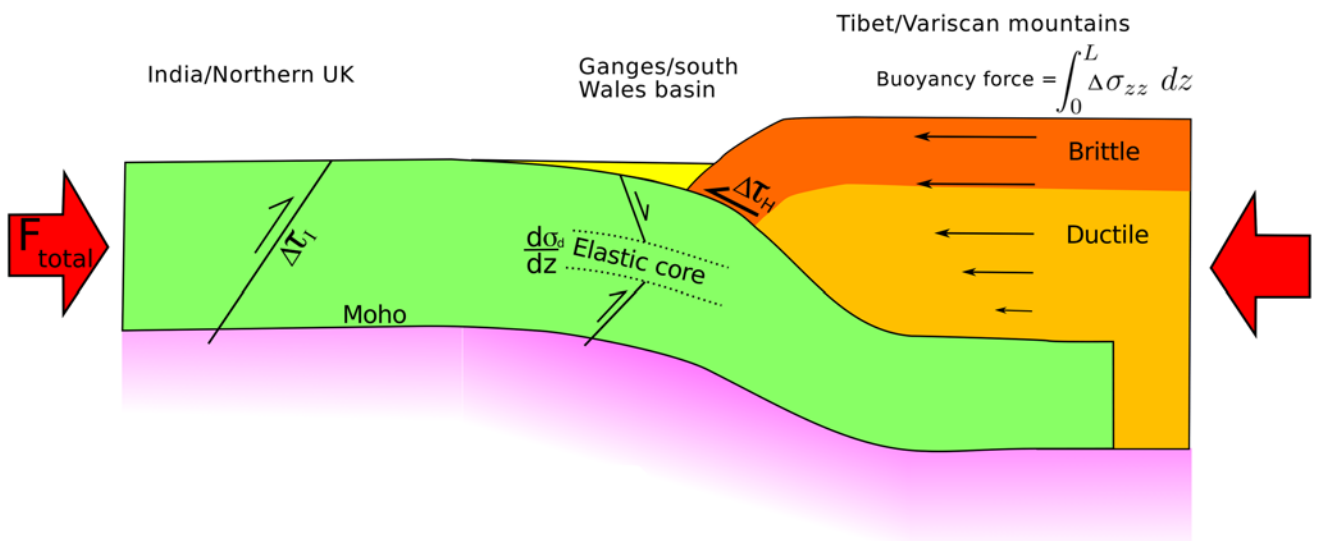


Fig. 3. A vertically exaggerated schematic illustration showing the constraints on fault strength that can be obtained from mountain ranges and their forelands, labelled with equivalent locations in the modern India–Asia collision zone and the northern margin of the Carboniferous Variscan mountain range. The green layer represents the underthrusting crust of the foreland (which thins as it enters the deformation belt, as it is partially incorporated into the overlying thrust belt). The dark orange layer is the seismogenic layer in the mountain range, and the pale orange layer is the viscous part. $\Delta\tau_1$ represents the stress drops in reverse faulting earthquakes in the foreland that are the result of the compressive forces exerted between the mountains and the lowlands (F_{total}). $\Delta\tau_H$ represents the stress drops in earthquakes on the range-bounding thrusts. The curvature of the underthrusting plate is controlled by the stress gradient in the elastic core ($d\sigma_d/dz$, where σ_d is the differential stress).

change orientation around the range, whereas those relating to the relative motions of the bounding plates will have roughly the same orientation along the length of the range. In some curved mountain ranges, such as southern Tibet, the slip direction in thrust earthquakes varies along the length of the range, and is everywhere perpendicular to the local strike of the mountain range. This configuration suggests that the gravitational potential energy contrasts dominate the deformation (Copley & McKenzie 2007). The magnitude of this force can be estimated from the crustal structure, allowing an upper limit to be placed on the amount of shear stress required to break the faults in earthquakes. In the Himalayas and Tibet, this upper limit is *c.* 50 MPa (blue shaded area in Fig. 1). This value represents an upper limit because the calculation assumes that no deviatoric stresses are supported in the ductile part of the lithosphere (i.e. that all the force transmitted between India and Tibet is supported by the dark orange layer in Fig. 3).

A similar argument was produced by Bollinger *et al.* (2004), who showed that the distribution and mechanisms of micro-seismicity in the Himalaya are related to the influence of the topography on the stress field. For the large thrusts that underlie the Himalaya to slip in response to this stress field implies slip at shear stresses ≤ 35 MPa ($\Delta\tau_H$ in Fig. 3). This estimate is compatible with the *c.* 10 MPa average stress drop in the 2015 M_w 7.8 Gorkha (Nepal) earthquake (e.g. Galetzka *et al.* 2015).

Lamb (2006) produced a global survey of subduction zones, and balanced the forces required to support the topography in the overriding plate with the stresses transmitted across the subduction interface. He found that the mean shear stresses on the subduction megathrusts were dominantly ≤ 15 MPa (equivalent to an effective coefficient of friction of ≤ 0.03), with the highest estimate being *c.* 35 MPa in the central Andes (yellow region in Fig. 1). These estimates rely on the topography in the overriding plate being close to the maximum elevation that can be supported by the stresses on the subduction interface, and so follows a similar logic to the work in the continents by Dalmayrac & Molnar (1981) and subsequent studies, which described the concept that the elevations of mountain plateaux could be used as a ‘pressure gauge’ to measure the magnitude of differential stress that can be supported by the lithosphere. These continental studies found similar values of vertically averaged crustal differential stresses of ≤ 50 MPa (e.g. Molnar & Lyon-Caen 1988; Copley *et al.* 2009).

Foreland force balance arguments

The final class of estimates of fault strength discussed here are those relating to the overall force balance in the forelands of mountain ranges and subduction zones, outboard of the megathrusts and flexural basins. In many areas of the world, both past and present, the apparently stable plate interiors adjacent to mountain ranges undergo slow but observable shortening in response to the compressive forces exerted between them and the neighbouring ranges. Earthquake source inversions, and geomorphological studies of ancient surface ruptures, allow the stress drops in the reverse-faulting earthquakes that accommodate the foreland shortening to be estimated ($\Delta\tau_1$ in Fig. 3; e.g. Seeber *et al.* 1996; Copley *et al.* 2011a, 2014). The total force that is exerted between India and Tibet (F_{total} in Fig. 3) can be estimated from force-balance calculations that aim to reproduce the direction and rate of motion of the Indian plate, and from estimates of the forces required to support the topography in Tibet (e.g. Copley *et al.* 2010). In central India, a failure envelope constructed from the stress drops in reverse-faulting earthquakes (red line in Fig. 1) implies that the faults support a similar vertically integrated force to the independently estimated total force exerted between India and Tibet (Copley *et al.* 2011a). This agreement suggests two conclusions. First, the faults

must be supporting the majority of the force transmitted through the Indian lithosphere (i.e. that the contribution of the ductile layer to the overall plate strength in this region is minor). Second, the stress drops in the earthquakes must represent almost all of the pre-earthquake shear stress on the faults, and so the faults must be able to support only a few tens of megapascals of shear stress before slipping in earthquakes. If the faults were significantly stronger than this (e.g. as predicted by Byerlee’s Law and hydrostatic pore fluid pressures), the available forces would be unable to cause the faults to rupture in earthquakes. Similar arguments can be made for other modern and ancient orogenic belts, and result in similar estimates of fault strength (e.g. as done by Copley & Woodcock 2016, for the Carboniferous Variscan mountain range).

Another location where earthquake source observations can be used to infer the stress state in the lithosphere is in the outer rises of subducting oceanic plates. Craig *et al.* (2014b) produced a global catalogue of outer-rise and trench-slope seismicity, and were able to determine the transition depth between shallow extension and deeper compression in a number of subduction zones. The curvature of an oceanic plate as it bends into a subduction zone depends upon the gradient of differential stress in the elastic core, between the shallow normal faults and deep reverse faults (e.g. McAdoo *et al.* 1978; the continental analogue is illustrated in Fig. 3). By combining bathymetric estimates of the curvature of subducting plates with the constraints on the thickness of the elastic core provided by earthquake mechanisms and depths, it is therefore possible to estimate the stress gradient within the elastic core, and the magnitude of the differential stresses that result in earthquake faulting. For the subduction zones where all of these observations were possible, Craig *et al.* (2014b) found that differential stresses of ≤ 300 MPa (equivalent to an effective coefficient of friction of ≤ 0.3) were sufficient to break the faults in earthquakes, but noted that this was an upper bound.

In contrast, a lower bound on fault strength can also be estimated in the oceans. Oceanic intraplate earthquakes, away from subduction-zone outer rises, are rare (and mainly confined to plate breakage along pre-existing weaknesses in regions subject to unusually large forces; e.g. Gordon *et al.* 1998; Robinson *et al.* 2001; Hill *et al.* 2015). This observation implies that in most of the world’s oceans, the magnitude of the ‘ridge push’ force is not sufficient to break the oceanic lithosphere. ‘Ridge push’ refers to the force arising from the lateral pressure differences between isostatically compensated ridges and older, cooler, oceanic lithosphere. Because the magnitude of this force depends only on the thermal structure of the oceanic lithosphere, which can be calculated from the age, it is the most well constrained in magnitude of the plate driving forces. Estimates for the force exerted between ridges and old oceanic lithosphere are $(2.5\text{--}3) \times 10^{12}$ N per metre along-strike (e.g. Parsons & Richter 1980). The 3×10^{12} N m^{-1} force contour is shown in bold in Figure 4. The seismogenic thickness in old oceanic lithosphere is 40–50 km (e.g. Craig *et al.* 2014b). Figure 4 therefore implies that the effective coefficient of friction in the oceanic lithosphere is ≥ 0.05 , otherwise pervasive intraplate deformation would be common in regions such as the Atlantic, where old seafloor flanks an active ridge.

Synthesis of observations

Is there one single view of fault strength that is consistent with all the observations and lines of logic described above? The lines of reasoning based upon force balances and strain orientations appear to require that, once formed, faults are able to break in earthquakes at shear stresses of megapascals to tens of megapascals, equivalent to an effective coefficient of friction of ≤ 0.3 . This view is also consistent with the thermal arguments, but raises two important questions. The first is whether these low stresses are due to high pore pressures or intrinsically weak fault rocks, and the second is how to

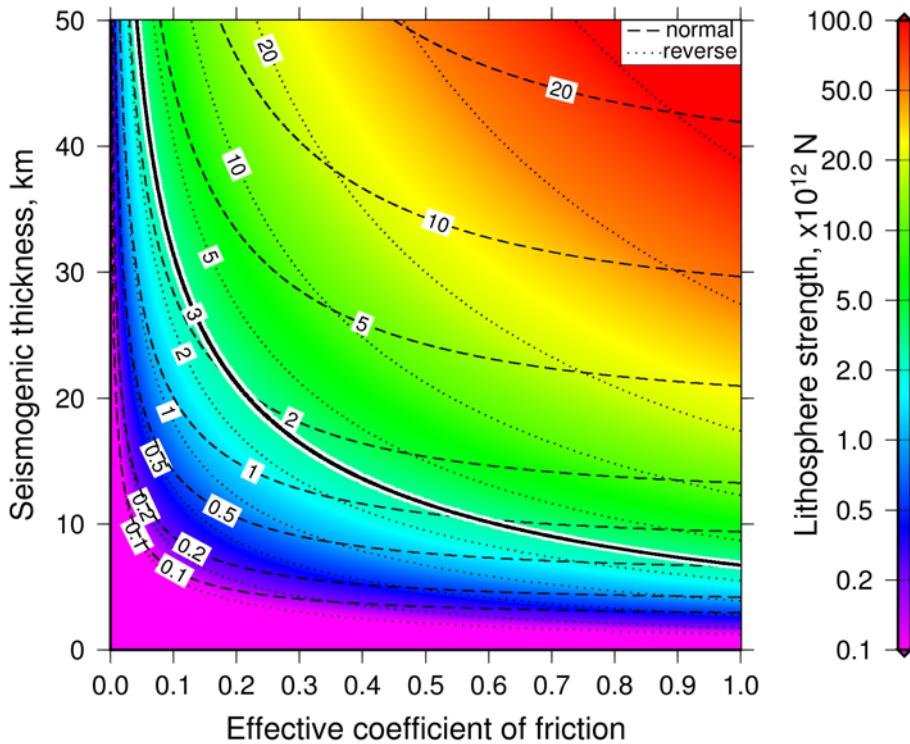


Fig. 4. The vertically integrated force that can be supported by the brittle upper lithosphere, as a function of the effective coefficient of friction and the thickness of the seismogenic layer. The dashed lines show values calculated for normal faulting, and the dotted lines for reverse faulting. The background is shaded according to the reverse-faulting values. Contours are labelled in units of 10^{12} N. The 3×10^{12} N contour for a reverse-faulting setting is shown in bold, and corresponds to the magnitude of the ‘ridge push’ force in the oceans (Parsons & Richter 1980).

reconcile these results with the laboratory and borehole studies that suggest much higher coefficients of friction.

Observations of fault dip distributions provide one means of distinguishing between pore pressure and mineralogical effects on fault friction. The dips at which faults are formed and reactivated should depend on only the intrinsic coefficient of friction of the rocks, and not the pore fluid pressure (e.g. Middleton & Copley 2014). The peak in seismogenic normal fault dips at close to 45° (Fig. 2) therefore implies intrinsically low-friction materials on the fault planes, presumably phyllosilicates (e.g. Byerlee 1978; Saffer *et al.* 2001; Brown *et al.* 2003). The formation and stability of these fault rocks will be discussed below. The geological observations of extensional veins produced by natural hydrofracture show that pore fluid pressures can also be locally high (e.g. Ramsay 1980; Sibson 1994; Robert *et al.* 1995; Barker *et al.* 2006), either consistently or transiently, and that the differential stresses when these features formed are therefore likely to be low (e.g. Etheridge 1983). It therefore seems likely that both weak minerals and high fluid pressures play a role in producing faults with a low effective coefficient of friction, although their relative importance and possible spatial or temporal variability are currently harder to address. Deep seismicity occurs in subducting slabs with similar stress drops to shallow events (e.g. Ye *et al.* 2013). At such depths, even coefficients of friction for phyllosilicates would predict unrealistically large forces to cause faulting, implying that high pore fluid pressures (possibly caused by metamorphic dehydration reactions; Raleigh 1967; Hacker *et al.* 2003) are crucial in this setting.

Laboratory experiments on fault rocks result in low estimates of the coefficient of friction that are similar to those inferred from the indirect methods discussed above. However, experiments on samples with an absence of interconnected phyllosilicates, and hydrofracture experiments in boreholes (which are based on the extensional fracture of intact rock, rather than inducing shear slip on pre-existing fault surfaces), imply much larger coefficients of friction. Combining these observations implies that faults with phyllosilicate-rich fault cores are embedded in intrinsically stronger unfaulted rock. This reasoning is consistent with observations that faults are often reactivated in non-optimal orientations during changes in tectonic regime, rather than new faults forming (e.g.

Sibson 1990; Masson 1991; Avouac *et al.* 2014; Copley & Woodcock 2016). However, this situation raises the questions of how fault zones form initially, in order to develop into persistent weaknesses, and how long this weakness can persist. These questions are discussed below.

If the low coefficients of friction of active faults are in part related to the presence of weak phyllosilicate-rich fault rocks, we must consider the conditions in which these minerals are stable. Based upon earthquake depth distributions, thermal models, field observations coupled with thermobarometry, and experimental results, rocks are thought to be able to break in earthquakes to temperatures of ~ 300 – 350°C in hydrous assemblages, and $\sim 600^\circ\text{C}$ in anhydrous settings (e.g. Kohlstedt *et al.* 1995; Lund *et al.* 2004; McKenzie *et al.* 2005; Jackson *et al.* 2008). This temperature contrast is likely to be due to the inefficiency of thermally activated creep mechanisms in anhydrous rocks, meaning that for a given strain-rate brittle failure can occur at lower differential stresses than ductile creep to greater temperatures (e.g. Mackwell *et al.* 1998; Jackson *et al.* 2008). Clay minerals form the cores of many exposed fault zones (e.g. Rutter *et al.* 1986; Faulkner *et al.* 2010), and the commonest of these (e.g. illites, smectites, kaolinites) react to form micas and chlorite at temperatures of 200 – 300°C (e.g. Frey 1978; Arkai 1991). In hydrous settings, these minerals could therefore be prevalent in fault zones through most or all of their depth range. Where faults break in earthquakes at temperatures of up to $\sim 600^\circ\text{C}$, it is likely that chlorite, micas, talc, or serpentine minerals will be the dominant phyllosilicates, provided that fluid flow along the faults can allow these hydrous minerals to form. Such a process is seen to happen in lower crustal rocks that were metamorphosed during the Caledonian Orogeny, where anhydrous granulites are transformed to hydrous eclogites by fluid influx along faults (e.g. Austrheim *et al.* 1997). However, for lower crustal earthquakes to occur at these elevated temperatures, where ductile creep would be expected in hydrous rocks, the degree of hydrous alteration must be small enough that the deformation is still by earthquake faulting in a dominantly anhydrous lower crust (e.g. Jackson *et al.* 2004). Such a situation may represent earthquakes nucleating at stress concentrations on the margins of pockets of weak phyllosilicates, and dynamically propagating into the surrounding anhydrous regions.

The low effective coefficients of friction discussed above are consistent with our knowledge of the forces involved in moving and deforming the tectonic plates. The $5.5 \pm 1.5 \text{ N m}^{-1}$ that India and Tibet exert upon each other is able to rupture faults that cut through the 40–50 km thick seismogenic layer of India, placing an upper bound on the effective coefficient of friction of $c. 0.1$ (Fig. 4; Copley *et al.* 2011a). An extension of this point is that because plate driving forces are generally thought to be in the range of $\leq 5 - 10 \text{ N m}^{-1}$ (e.g. Forsyth & Uyeda 1975; Parsons & Richter 1980; Molnar & Lyon-Caen 1988; Conrad & Hager 1999; Copley *et al.* 2010), the presence of active faulting in regions where the distribution of earthquakes shows the seismogenic layer is $\geq 40 \text{ km}$ thick (e.g. Assumpcao & Suarez 1988; Craig *et al.* 2011) means that the results regarding India must be generally applicable to such regions, and the effective coefficient of friction must be ≤ 0.2 (Fig. 4).

In contrast, some areas of the plate interiors show no clear signs of significant deformation, which can be interpreted in two ways. Where sparse microseismicity implies a low seismogenic thickness (e.g. $\leq 20 \text{ km}$ in the UK; Baptie 2010), the lack of deformation is likely to be the result of low levels of differential stress. Such a situation could arise because of, for example, the buoyancy force acting across continental margins balancing the ridge push force arising from the cooling of the adjacent oceanic lithosphere (e.g. Le Pichon & Sibuet 1981; Pascal & Cloetingh 2009). However, some undeforming regions of the continents presumably are subject to

significant forces, such as stable Eurasia, which experiences approximately the same forces resulting from the construction of the Alpine–Himalayan belt as does deforming India to the south. In these regions the lack of deformation is likely to be due to the lithosphere being cool and chemically depleted enough that the seismogenic layer is so thick that even for low coefficients of friction the forces acting on the plates are too small to cause faulting (Fig. 4).

Simple calculations can be used to assess whether estimates of fault strength are consistent with the rates of plate motion. The results described above imply that differential stresses of tens of megapascals can be transmitted across faults on the lateral boundaries of plates. These stresses will be balanced by tractions on the base of the plates, which depend upon the rate of motion relative to the underlying mantle, and the thickness and viscosity of the layer in which this motion is accommodated. A variety of observations and models have suggested that the plate motions are accommodated by shearing in the asthenosphere, with a thickness of $c. 100 - 200 \text{ km}$ and a viscosity of $\sim 10^{18} - 10^{19} \text{ Pa s}$ (e.g. Craig & McKenzie 1986; Hager 1991; Fjeldskaar 1994; Goumelen & Amelung 2005; Copley *et al.* 2010). For these parameters, if the plates are thousands to tens of thousands of kilometres wide, then they must move at rates of the order of centimetres to tens of centimetres per year for the tractions on the base to balance the forces transmitted across faults on their lateral edges, in agreement

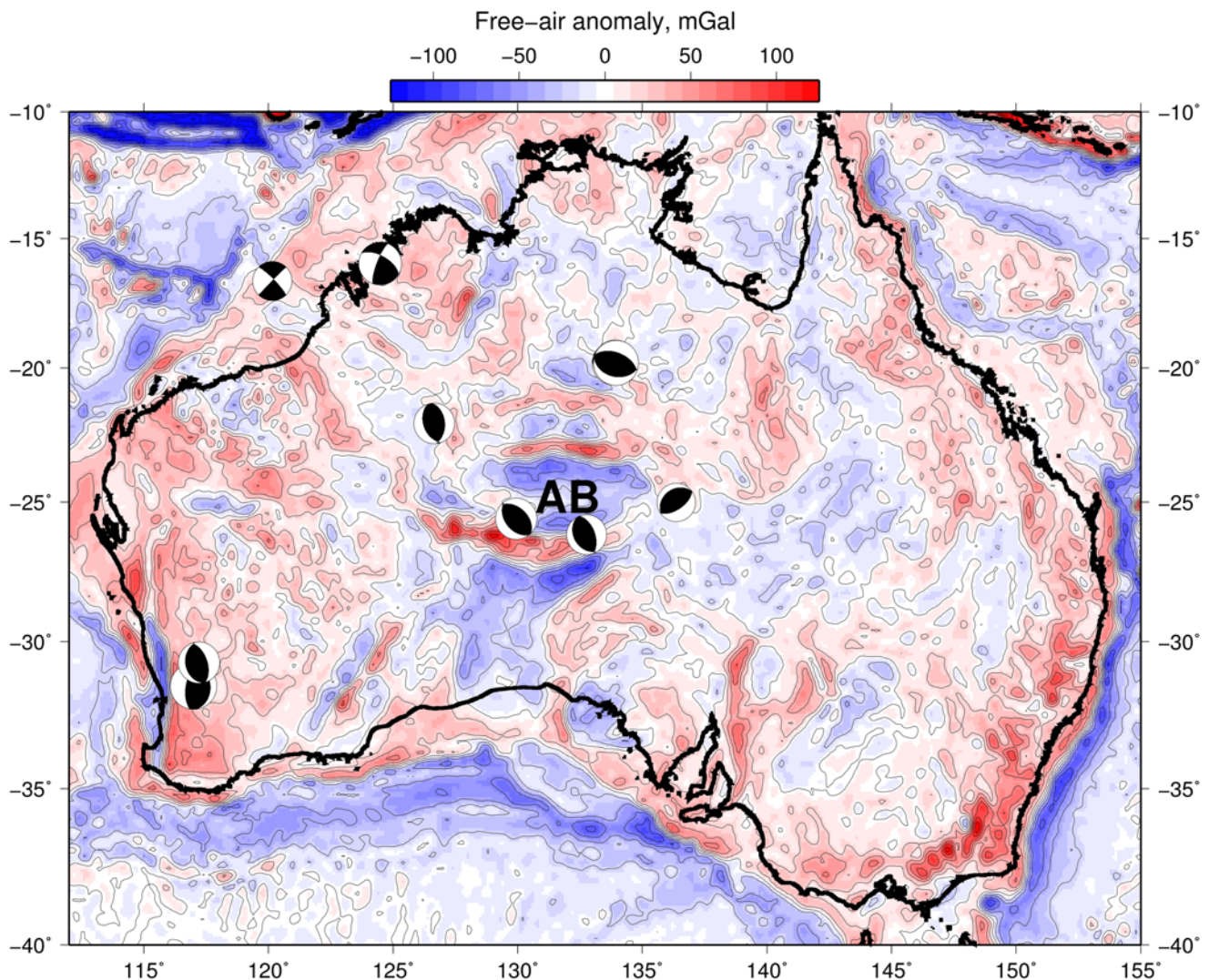


Fig. 5. Free-air gravity anomalies in Australia, from the Eigen-6C model of Forste *et al.* (2011), contoured at 20 mGal intervals. Also shown are the mechanisms of earthquakes of $M_w \geq 5.5$ and larger, from Fredrich *et al.* (1988), McCaffrey (1989) and the global CMT project. AB, Amadeus Basin.

with observations. More detailed force-balance calculations for single plates confirm this pattern (e.g. Copley *et al.* 2010; Warners-Ruckstuhl *et al.* 2012).

Open questions

The discussion above has raised two important questions that have yet to be fully answered. It seems apparent that faults that have undergone enough slip to generate phyllosilicate-rich fault cores are considerably weaker than unfaulted rock. This amount of slip could be as little as tens of metres, depending on lithology (e.g. Lacroix *et al.* 2015). If the differential stresses in the lithosphere are limited by these pre-existing faults, this result raises the question of how new faults are formed. One possibility is that high pore fluid pressures, close to lithostatic, are required to initiate new faults. A second possibility is that faults simply propagate along-strike, driven by large stress concentrations at the ends of already existing structures. This second mechanism clearly requires an explanation for the formation of these existing features, but minimizes the rate at which new structures are required to form, and so the prevalence of the required conditions. The difficulties in identifying regions of new fault formation, and mapping the ordering of fault development, mean that the mechanism of initiation is still unknown. New faults forming in the outer rises of subduction zones do so at an angle that implies a low intrinsic coefficient of friction (Craig *et al.* 2014a), but it remains to be established whether this observation represents faults nucleating in regions where mid-ocean ridge hydrothermal alteration has left a pre-existing network of weak phyllosilicates, or whether these results imply a lack of applicability of the laboratory and borehole measurements to those tectonic conditions.

A final open question concerns fault healing through time. In some continental interiors, large gravity anomalies are present that were formed by juxtaposing rocks of different densities during previous phases of faulting. One example is central Australia, which contains some of the largest gravity anomalies in the continental interiors (Fig. 5). These anomalies, running east–west and flanking the Amadeus Basin (AB in Fig. 5), have been produced by repeated phases of deformation, the most recent being shortening at 300–400 Ma (e.g. Shaw *et al.* 1991). The present-day gravity anomalies require forces of $\geq 4 \times 10^{12} \text{ N m}^{-1}$ to be supported, equivalent to vertically averaged differential stresses of *c.* 100–200 MPa (e.g. Stephenson & Lambeck 1985). Such forces are significantly higher than those able to break faults in the world's deformation zones, as discussed above. Faults are clearly present in the region of the central Australian gravity anomalies, as these anomalies were produced by faulting, and the same deformation zones were repeatedly active in the Proterozoic and Palaeozoic (Shaw *et al.* 1991). However, there is no evidence of these faults being active at resolvable rates at the present day. The earthquake focal mechanisms in Figure 5 show that some of the present-day reverse-faulting in central Australia is at angles perpendicular to that which would be expected to result from the forces required to support the gravity anomalies, showing that these forces do not drive the deformation. These observations imply that faults must be able to heal over time, and recover a strength more similar to intact rock. Whether this healing is accomplished by solution and precipitation in the fault zones (e.g. Angevine *et al.* 1982; Olson *et al.* 1998; Tenthorey *et al.* 2003; Yasuhara *et al.* 2005), metamorphic dehydration reactions producing a strong anhydrous substrate beneath the faults (e.g. Mackwell *et al.* 1998; Lund *et al.* 2004), or some other mechanism, and the time and conditions required for these processes to occur, remain open questions. Equally, it is not yet understood why these processes should occur in some places, whereas in other continental interiors inherited Proterozoic deformation belts still represent weaknesses that govern the geometry of the active deformation, by

either brittle reactivation or the control of fault geometries by Proterozoic ductile foliations (e.g. in East Africa and India; Versfelt & Rosendahl 1989; Ring 1994; Ebinger *et al.* 1997; Talwani & Gangopadhyay 2001; Chorowicz 2005).

Conclusions

The conceptual view most consistent with all available observations and inferences of fault strength is that a combination of intrinsically low-friction minerals (e.g. phyllosilicates) and high pore fluid pressures results in a network of weak faults cutting through the surrounding strong rocks. These faults can slip at shear stresses of ≤ 50 MPa, corresponding to effective coefficients of friction of 0.05–0.3, and are at least 30% weaker than unfaulted rock. Major questions remaining to be answered in this subject area include the conditions required for the formation of new faults, and the mechanisms, causes and consequences of fault healing through time.

Acknowledgements The author wishes to thank C. Penney, S. Wimpenny and J. Jackson for comments on the paper, and A. Fagerang and an anonymous reviewer for helpful reviews.

Funding This work forms part of the NERC- and ESRC-funded project 'Earthquakes without Frontiers', and was partly supported by the NERC grant 'Looking Inside the Continents from Space'.

Scientific editing by Carl Stevenson

References

- Allmann, B.P. & Shearer, P.M. 2009. Global variations of stress drop for moderate to large earthquakes. *Journal of Geophysical Research*, **114**, <https://doi.org/10.1029/2008JB005821>
- Ambraseys, N.N. & Jackson, J.A. 1998. Faulting associated with historical and recent earthquakes in the Eastern Mediterranean region. *Geophysical Journal International*, **133**, 390–406.
- Anderson, E.M. 1951. *The Dynamics of Faulting*, 2nd edn. Oliver & Boyd, Edinburgh.
- Angevine, C.L., Turcotte, D.L. & Furnish, M.D. 1982. Pressure solution lithification as a mechanism for the stick–slip behaviour of faults. *Tectonics*, **1**, 151–160.
- Arkai, P. 1991. Chlorite crystallinity: an empirical approach and correlation with illite crystallinity, coal rank and mineral facies as exemplified by Palaeozoic and Mesozoic rocks of northeast Hungary. *Journal of Metamorphic Geology*, **9**, 723–734.
- Artyushkov, E.V. 1973. Stresses in the lithosphere caused by crustal thickness inhomogeneities. *Journal of Geophysical Research*, **78**, 7675–7708.
- Assumpcao, M. & Suarez, G. 1988. Source mechanisms of moderate-sized earthquake and stress orientation in mid-plate South America. *Geophysical Journal International*, **92**, 253–267.
- Austrheim, H., Erambert, M. & Engvik, A.K. 1997. Processing of crust in the root of the Caledonian continental collision zone: the role of eclogitization. *Tectonophysics*, **273**, 129–153.
- Avouac, J.-P., Ayoub, F. *et al.* 2014. The 2013, Mw 7.7 Balochistan earthquake, energetic strike-slip reactivation of a thrust fault. *Earth and Planetary Science Letters*, **391**, 128–134.
- Baptie, B. 2010. Seismogenesis and state of stress in the UK. *Tectonophysics*, **482**, 150–159.
- Barker, S.L.L., Cox, S.F., Eggins, S.M. & Gagan, M.K. 2006. Microchemical evidence for episodic growth of anitaxial veins during fracture-controlled fluid flow. *Earth and Planetary Science Letters*, **250**, 331–344.
- Beach, A. 1980. Retrogressive metamorphic processes in shear zones with special reference to the Lewisian complex. *Journal of Structural Geology*, **2**, 257–263.
- Beck, S., Barrientos, S., Kausel, E. & Reyes, M. 1998. Source characteristics of historic earthquakes along the central Chile subduction zone. *Journal of South American Earth Sciences*, **11**, 115–129.
- Bollinger, L., Avouac, J.P., Cattin, R. & Pandey, M.R. 2004. Stress buildup in the Himalaya. *Journal of Geophysical Research*, **109**, <https://doi.org/10.1029/2003JB002911>
- Brown, K.M. & Fialko, Y. 2012. 'Melt welt' mechanism of extreme weakening of gabbro at seismic slip rates. *Nature*, **488**, 638–641.
- Brown, K.M., Kopf, A., Underwood, M.B. & Weinberger, J.L. 2003. Compositional and fluid pressure controls on the state of stress on the Nankai subduction thrust: A weak plate boundary. *Earth and Planetary Science Letters*, **214**, 589–603.

The strength of earthquake-generating faults

- Lamb, S. 2006. Shear stresses on megathrusts: Implications for mountain building behind subduction zones. *Journal of Geophysical Research*, **111**, <https://doi.org/10.1029/2005JB003916>
- Le Pichon, X. & Sibuet, J.-C. 1981. Passive margins: A model of formation. *Journal of Geophysical Research*, **86**, 3708–3720.
- Li, H., Xue, L. *et al.* 2015. Long-term temperature records following the Mw 7.9 Wenchuan (China) earthquake are consistent with low friction. *Geology*, **43**, 163–166.
- Lockner, D.A., Morrow, C., Moore, D. & Hickman, S. 2011. Low strength of deep San Andreas fault gouge from SAFOD core. *Nature*, **472**, 82–85.
- Lund, B. & Zoback, M.D. 1999. Orientation and magnitude of *in situ* stress to 6.5 km depth in the Baltic Shield. *International Journal of Rock Mechanics and Mining Sciences*, **36**, 169–190.
- Lund, M.G., Austrheim, H. & Erambert, M. 2004. Earthquakes in the deep continental crust – insights from studies on exhumed high-pressure rocks. *Geophysical Journal International*, **158**, 569–576.
- Mackwell, S.J., Zimmerman, M.E. & Kohlstedt, D.L. 1998. High temperature deformation of dry diabase with application to the tectonics of Venus. *Journal of Geophysical Research*, **103**, 975–984.
- Marone, C. 1998. Laboratory-derived friction laws and their application to seismic faulting. *Annual Review of Earth and Planetary Sciences*, **26**, 643–696.
- Masson, D.G. 1991. Fault patterns at outer trench walls. *Marine Geophysical Researches*, **13**, 209–225.
- McAdoo, D.C., Caldwell, J.G. & Turcotte, D.L. 1978. On the elastic–perfectly plastic bending of the lithosphere under generalized loading with application to the Kuril Trench. *Geophysical Journal of the Royal Astronomical Society*, **54**, 11–26.
- McCaffrey, R. 1989. Teleseismic investigation of the January 22, 1988 Tennant Creek, Australia, earthquakes. *Geophysical Research Letters*, **16**, 413–416.
- McGarr, A. 1999. On relating apparent stress to the stress causing earthquake fault slip. *Journal of Geophysical Research*, **104**, 3001–3011.
- McKenzie, D.P. 1969. The relation between fault plane solutions for earthquakes and the directions of the principal stresses. *Bulletin of the Seismological Society of America*, **59**, 591–601.
- McKenzie, D. & Brune, J.N. 1972. Melting on fault planes during large earthquakes. *Geophysical Journal of the Royal Astronomical Society*, **29**, 65–78.
- McKenzie, D., Jackson, J. & Priestley, K. 2005. Thermal structure of oceanic and continental lithosphere. *Earth and Planetary Science Letters*, **233**, 337–349.
- Middleton, T.A. & Copley, A. 2014. Constraining fault friction by re-examining earthquake nodal plane dips. *Geophysical Journal International*, **196**, 671–680.
- Miller, G.G. 1998. Distributed shear, rotation, and partitioned strain along the San Andreas fault, central California. *Geology*, **26**, 867–870.
- Molnar, P. & Lyon-Caen, H. 1988. Some simple physical aspects of the support, structure, and evolution of mountain belts. In: Clark, S.P., Burchfiel, B.C. & Suppe, J. (eds) *Processes in Continental Lithospheric Deformation*. Geological Society of America, Special Papers, **218**, 179–207.
- Mount, V.S. & Suppe, J. 1987. State of stress near the San Andreas fault: Implications for wrench tectonics. *Geology*, **15**, 1143–1146.
- Noda, H. & Lapusta, N. 2013. Stable creeping fault segments can become destructive as a result of dynamic weakening. *Nature*, **493**, 518–521.
- Olson, M.P., Scholz, C.H. & Leger, A. 1998. Healing and sealing of a simulated fault gouge under hydrothermal conditions: Implications for fault healing. *Journal of Geophysical Research*, **103**, 7421–7430.
- Osborne, M.J. & Swarbrick, R.E. 1997. Mechanisms for generating overpressure in sedimentary basins; a reevaluation. *AAPG Bulletin*, **81**, 1023–1041.
- Parsons, B. & Richter, F.M. 1980. A relation between the driving force and geoid anomaly associated with mid-ocean ridges. *Earth and Planetary Science Letters*, **51**, 445–450.
- Pascal, C. & Cloetingh, S.A.P.L. 2009. Gravitational potential stresses and stress field of passive continental margins: Insights from the south-Norway shelf. *Earth and Planetary Science Letters*, **277**, 464–473.
- Raleigh, C.B. 1967. Tectonic implications of serpentinite weakening. *Geophysical Journal of the Royal Astronomical Society*, **14**, 113–118.
- Ramsay, J.G. 1980. The crack-seal mechanism of rock deformation. *Nature*, **284**, 135–139.
- Reches, Z. & Lockner, D.A. 2010. Fault weakening and earthquake instability by powder lubrication. *Nature*, **467**, 452–455.
- Remitti, F., Smith, S.A.F., Mitterperger, S., Gualtieri, A.F. & Di Toro, G. 2015. Frictional properties of fault zone gouges from the J-FAST drilling project (Mw 9.0 2011 Tohoku–Oki earthquake). *Geophysical Research Letters*, **42**, 2691–2699.
- Rice, J.R. 2006. Heating and weakening of faults during earthquake slip. *Journal of Geophysical Research*, **111**, <https://doi.org/10.1029/2005JB004006>
- Ring, U. 1994. The influence of preexisting structure on the evolution of the Cenozoic Malawi rift (East African rift system). *Tectonics*, **13**, 313–326.
- Robert, F., Boullier, A.-M. & Firdaus, K. 1995. Gold–quartz veins in metamorphic terranes and their bearing on the role of fluids in faulting. *Journal of Geophysical Research*, **100**, 12861–12879.
- Robinson, D., Henry, C., Das, S. & Woodhouse, J.H. 2001. Simultaneous rupture along two conjugate planes of the Wharton Basin earthquake. *Science*, **292**, 1145–1148.
- Rona, P.A., Klinkhammer, G., Nelson, T.A., Trefry, J.H. & Elderfield, H. 1986. Black smokers, massive sulphides and vent biota at the Mid-Atlantic Ridge. *Nature*, **321**, 33–37.
- Ruina, A. 1983. Slip instability and state variable friction laws. *Journal of Geophysical Research*, **88**, 10359–10370.
- Rutter, E.H., Maddock, R.H., Hall, S.H. & White, S.H. 1986. Comparative microstructures of natural and experimentally produced clay-bearing fault gouges. *Pure and Applied Geophysics*, **124**, 3–30.
- Saffer, D.M., Frye, K.M., Marone, C. & Mair, K. 2001. Laboratory results indicating complex and potentially unstable frictional behaviour of smectite clay. *Geophysical Research Letters*, **28**, 2297–2300.
- Scholz, C.H. 1990. *The Mechanics of Earthquakes and Faulting*, 1st edn. Cambridge University Press, Cambridge.
- Scholz, C.H. 1998. Earthquakes and friction laws. *Nature*, **391**, 37–42.
- Scholz, S.Y. 1999. Noncharacteristic behavior and complex recurrence of large subduction zone earthquake. *Journal of Geophysical Research*, **104**, 23111–23125.
- Scholz, C.H. 2000. Evidence for a strong San Andreas fault. *Geology*, **28**, 163–166.
- Scott, J.S. & Drever, H.I. 1954. Frictional heating along a Himalayan thrust. *Proceedings of the Royal Society of Edinburgh, Section B*, **65**, 121–142.
- Secor, D.T. 1965. Role of fluid pressure in jointing. *American Journal of Science*, **263**, 633–646.
- Seeber, L., Ekstrom, G., Jain, S.K., Murty, C.V.R., Chandak, N. & Armbruster, J. G. 1996. The 1993 Killari earthquake in central India: A new fault in Mesozoic basalt flows? *Journal of Geophysical Research*, **101**, 8543–8560.
- Shaw, R.D., Etheridge, M.A. & Lambeck, K. 1991. Development of the late Proterozoic to mid-Palaeozoic, intracratonic Amadeus Basin in central Australia: A key to understanding tectonic forces in plate interiors. *Tectonics*, **10**, 688–721.
- Sibson, R.H. 1975. Generation of pseudotachylite by ancient seismic faulting. *Geophysical Journal of the Royal Astronomical Society*, **43**, 775–794.
- Sibson, R.H. 1977. Fault rocks and fault mechanisms. *Journal of the Geological Society, London*, **133**, 191–213, <https://doi.org/10.1144/gsjgs.133.3.0191>
- Sibson, R.H. 1985. A note on fault reactivation. *Journal of Structural Geology*, **7**, 751–754.
- Sibson, R.H. 1990. Rupture nucleation on unfavorably oriented faults. *Bulletin of the Seismological Society of America*, **90**, 1580–1604.
- Sibson, R.H. 1994. Crustal stress, faulting, and fluid flow. In: Parnell, J. (ed.) *Geofluids: Origin, Migration and Evolution of Fluids in Sedimentary Basins*. Geological Society, London, Special Publications, **78**, 69–84, <https://doi.org/10.1144/GSL.SP.1994.078.01.07>
- Sibson, R.H. 2004. Controls on maximum fluid overpressure defining conditions for mesozonal mineralisation. *Journal of Structural Geology*, **26**, 1127–1136.
- Sibson, R.H. 2014. Earthquake rupturing in fluid-overpressured crust: How common? *Pure and Applied Geophysics*, **171**, 2867–2855.
- Sibson, R.H. & Toy, V.G. 2006. The habitat of fault-generated pseudotachylite: presence vs. absence of friction-melt. In: *Radiated Energy and the Physics of Faulting*. American Geophysical Union, Geophysical Monograph, **170**, 153–166.
- Sibson, R.H. & Xie, G. 1998. Dip range for intracontinental reverse fault ruptures: Truth not stranger than friction? *Bulletin of the Seismological Society of America*, **88**, 1014–1022.
- Sieh, K., Natawidjaja, D.H. *et al.* 2008. Earthquake supercycles inferred from the sea-level changes recorded in the corals of west Sumatra. *Science*, **322**, 1674–1678.
- Sleep, N.H. & Blanpied, M.L. 1992. Creep, compaction and weak rheology of major faults. *Nature*, **359**, 687–692.
- Smith, J.E. 1971. The dynamics of shale compaction and evolution of pore-fluid pressures. *Mathematical Geology*, **2**, 239–263.
- Spray, J.G. 1993. Viscosity determinations of some frictionally generated silicate melts: Implications for fault zone rheology at high strain rates. *Journal of Geophysical Research*, **98**, 8053–8068.
- Stephenson, R. & Lambeck, K. 1985. Isostatic response of the lithosphere with in-plane stress: Application to Central Australia. *Journal of Geophysical Research*, **90**, 8581–8588.
- Steward, T.M. 1993. The hydrothermal geochemistry of gold. In: Foster, B. (ed.) *Gold Metallurgy and Exploration*. Springer, Berlin, 37–62.
- Talwani, P. & Gangopadhyay, A. 2001. Tectonic framework of the Kachchh earthquake of January 26, 2001. *Seismological Research Letters*, **72**, 336–345.
- Taymaz, T., Jackson, J. & McKenzie, D. 1991. Active tectonics of the north and central Aegean Sea. *Geophysical Journal International*, **106**, 433–490.
- Tenthorey, E., Cox, S.F. & Todd, H.F. 2003. Evolution of strength recovery and permeability during fluid–rock reaction in experimental fault zones. *Earth and Planetary Science Letters*, **206**, 161–172.
- Thatcher, W. & Hill, D.P. 1991. Fault orientations in extensional and conjugate strike-slip environments and their implications. *Geology*, **19**, 1116–1120.
- Townend, J. & Zoback, M.D. 2000. How faulting keeps the crust strong. *Geology*, **28**, 399–402.
- Versfelt, J. & Rosendahl, B.R. 1989. Relationships between pre-rift structure and rift architecture in Lakes Tanganyika and Malawi, East Africa. *Nature*, **337**, 354–357.
- Walther, J.V. & Orville, P.M. 1982. Volatile production and transport in regional metamorphism. *Contributions to Mineralogy and Petrology*, **79**, 252–257.

- Warners-Ruckstuhl, K.N., Govers, R. & Wortel, R. 2012. Lithosphere–mantle coupling and the dynamics of the Eurasian Plate. *Geophysical Journal International*, **189**, 1253–1276.
- Watts, A.B. & Burov, E.B. 2003. Lithospheric strength and its relationship to the elastic and seismogenic layer thickness. *Earth and Planetary Science Letters*, **213**, 113–131.
- Wintsch, R.P., Christoffersen, R. & Kronenberg, A.K. 1995. Fluid–rock reaction weakening of fault zones. *Journal of Geophysical Research*, **100**, 13021–13032.
- Yardley, B.W.D. 2009. The role of water in the evolution of the continental crust. *Journal of the Geological Society, London*, **116**, 585–600, <https://doi.org/10.1144/0016-76492008-101>
- Yasuhara, H., Marone, C. & Elsworth, D. 2005. Fault zone restrengthening and frictional healing: The role of pressure solution. *Journal of Geophysical Research*, **110**, <https://doi.org/10.1029/2004JB003327>
- Ye, L., Lay, T., Kanamori, H. & Koper, K.D. 2013. Energy release of the 2013 Mw 8.3 Sea of Okhotsk earthquake and deep slab stress heterogeneity. *Science*, **341**, 1380–1384.
- Zoback, M.D. & Healy, J.H. 1992. *In situ* stress measurements to 3.5 km depth in the Cajon Pass Scientific Research Borehole: implications for the mechanics of crustal faulting. *Journal of Geophysical Research*, **97**, 5039–5057.
- Zoback, M.D., Barton, C.A. *et al.* 2003. Determination of stress orientation and magnitude in deep wells. *International Journal of Rock Mechanics and Mining Sciences*, **40**, 1049–1076.